Ecotoxicology and Environmental Safety 306 (2025) 119287

Contents lists available at ScienceDirect

Ecotoxicology and Environmental Safety

journal homepage: www.elsevier.com/locate/ecoenv

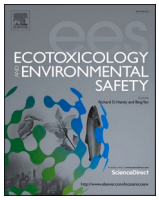

Synergistic effects of biochar and phosphate fertilizer on fungal communities and soybean productivity in microplastic-contaminated alkaline soils

Min Sun, Xiao-Yu Li, Hai-Yan Yuan *, Qi-Lu Zhuang, Huan-Guang Deng, Bao-Xian Tao, Bao-Hua Zhang *

School of Geography and Environment, Liaocheng University, Liaocheng 252000, China

A R T I C L E I N F O

Edited by Dr Yong Liang

Keywords:
Low-density polyethylene microplastics (LDPE-MPs)
Alkaline soil
Biochar-fertilizer integration
Phosphorus bioavailability
Microbial activity

A B S T R A C T

Alkaline soils suffer from phosphorus (P) bioavailability limitations due to fixation and precipitation, which is further exacerbated by microplastics (MPs) disrupting plant-microbe-soil P dynamics and threatening crop productivity. This study investigated the synergistic effects of applying 2 % (w/w) maize-derived biochar (a soil amendment that enhances nutrient retention and microbial activity) and varying phosphate fertilizers (0–180 kg P ha^{-1}) in MPs-contaminated alkaline soils. Comprehensive investigations were conducted on the effects of the combined addition of phosphate fertilizer and biochar on P dynamics, fungal communities, and soybean growth. Results showed that biochar significantly reshaped soil fungal community structure and composition by modulating pH, nutrient availability, and organic matter dynamics, while increasing *Aspergillus* and *Fusarium* abundance, which play a key role in phosphorus solubilization and pollutant degradation. Additionally, co-occurrence network analysis revealed that applying biochar enhanced network complexity, promoted negative interactions, and intensified interspecific competition within the rhizosphere fungal community. Notably, the combined application of biochar with moderate-level P fertilization (60 kg P ha^{-1}, 90 kg P ha^{-1}) increased soybean total biomass (40.73 %, 42.58 %), total P uptake (58.19 %, 34.44 %), and yield (74.38 %, 84.16 %), indicating improved P-use efficiency. Additionally, Partial Least Squares Path Modeling (PLS-PM) revealed that the rhizosphere effect promoted soybean P uptake by regulating nutrient cycling, thereby enhancing yield. These findings provide critical insights into sustainable agriculture under dual challenges of MPs pollution and limited P resources, contributing scientific and efficient strategies for nutrient management and rational P fertilizer use in resource-constrained agroecosystems.

1. Introduction

Low-density polyethylene (LDPE)-based plastic films are widely utilized in agricultural practices, playing crucial roles in preserving soil moisture, suppressing weed proliferation, and modulating temperature (Niroshika et al., 2022). It is reported that the annual consumption of mulching and greenhouse films has surpassed two million tons in China (Ma et al., 2024). Plastic films accumulate persistently owing to sub-optimal recovery efficiency and non-biodegradability (Palansooriya et al., 2023). Undergoing physical, chemical, and biological processes, the residue progressively decomposes into fragments smaller than 5 mm, known as microplastics (MPs) (Thompson et al., 2004). MPs have garnered global attention considering their widespread occurrence in agricultural ecosystems and potential consequences for soil health and agricultural productivity. As an illustration, Li et al. (2021) demonstrated that LDPE negatively affected soybean growth by reducing leaf area, stalk diameter, plant height, and root-to-shoot ratio. Furthermore, LDPE remarkably altered soil bacterial community structure and succession, while also stimulating soil enzymatic activities and increasing the prevalence of functional genes associated with nitrogen cycling (Feng et al., 2024). It is projected that by 2050, the globally accumulated polyethylene waste will reach 270 million tons (Zhang et al., 2025), highlighting the necessity for assessing its potential hazards to the agricultural ecosystem.

Alkaline soils with high pH levels and elevated exchangeable sodium percentages represent a valuable agricultural resource. Nevertheless,

* Corresponding authors.
E-mail addresses: hyyuan@lcu.edu.cn (H.-Y. Yuan), zhangbaohua@lcu.edu.cn (B.-H. Zhang).

https://doi.org/10.1016/j.ecoenv.2025.119287
Received 25 August 2025; Received in revised form 5 October 2025; Accepted 21 October 2025
Available online 27 October 2025

they are frequently constrained by significant nutrient deficiencies (including cations, micronutrients, and phosphorus) and/or sodium toxicity, resulting in problems like restricted rate of litter decomposition, nutrient depletion, and decreased microbial activity (Byrt et al., 2023). Phosphorus (P) is one of the most limiting nutrients for plants and pivotal to biomolecule synthesis and physiological process regulation (Mo et al., 2022). However, the bioavailability of phosphorus is often constrained by its tendency to bind with mineral elements and form insoluble compounds in alkaline soils, which makes agricultural production highly dependent on mineral fertilizers to meet crop nutrient requirements (Chen et al., 2019). Globally, approximately 16.4 Tg of phosphate fertilizers are applied annually to support agricultural production (Gong et al., 2022). Nonetheless, due to adsorption, precipitation, and microbial activity, 70–90 % of applied phosphorus becomes trapped in the soil, decreasing its accessibility to plants and limiting crop growth (Xu et al., 2024). Moreover, excessive and prolonged use of phosphate fertilizers not only causes input-output inefficiencies but also leads to depletion of rock phosphate resources, water eutrophication, and biodiversity loss (Chen et al., 2025; Chen et al., 2021). Few studies have explored the effects of microplastics on plant phosphorus uptake and soil phosphorus transformation in alkaline soils, where phosphorus bioavailability is already inherently low due to mineral binding. Therefore, further clarification of the interaction mechanisms between microplastics and phosphorus behavior in alkaline soil systems is needed, as is the development of sustainable agricultural strategies that optimize phosphorus use while mitigating microplastic pollution.

Biochar, which is typically formed by carbonizing biomass under anaerobic conditions, has been recognized as a prospective soil amendment on account of its high carbon content, adsorption potential, and capability to improve soil health, stimulate plant growth, and ameliorate greenhouse gas emissions (Liao et al., 2023; Zhang et al., 2025). Studies have demonstrated that biochar, which can supply available nutrients (N, P, and K) or modify soil physicochemical attributes (e.g., cation exchange capacity, pH, and phosphorus sorption potential), in turn directly or indirectly affects phosphorus speciation and accessibility (Hossain et al., 2020; Shi et al., 2023). Furthermore, microorganisms make a significant contribution to phosphorus mineralization by releasing inorganic phosphorus from intractable substrates and secreting enzymes (e.g., phosphatases and phytases) (Huang et al., 2021; Wang et al., 2024). Integrating biochar into the soil can promote the overall phosphorus accessibility by providing a favorable biotope for P-mobilizing microorganisms (Deinert et al., 2024). These findings accentuate its potential to improve soil phosphorus availability.

Soybean, a vital crop with high nutritional value, provides edible oil and protein for humans and serves as livestock feed, making it a cornerstone of agricultural production (Fang et al., 2024). The global demand for soybean products is steadily increasing, with projections estimating a demand of 133 million tons by 2035 (Guo et al., 2022). Nonetheless, China's soybean production capacity is relatively weak, with approximately 83 % of its consumption relying on imports, posing significant challenges to the soybean industry (Wang et al., 2024). As a phosphorus-demanding crop, soybean requires substantial phosphorus during growth, and insufficient phosphorus disrupts root growth, inhibits phosphorus transport, and diminishes plant phosphorus content (Li et al., 2022; Liu et al., 2024). Moreover, MPs could disrupt soil available phosphorus concentration, further exacerbating the phosphorus stress faced by soybean during growth (Liu et al., 2023). Faced with the dual stress of phosphorus deficiency and microplastic pollution, we hypothesized that combining biochar amendment with phosphate fertilizer application could ameliorate the negative impacts of microplastic pollution and boost phosphorus bioavailability by improving soil physicochemical properties, stabilizing microbial community stability, and promoting overall soybean growth. To test this hypothesis, a controlled experiment was performed to (i) evaluate the synergistic effects of biochar and phosphate fertilizer for agricultural potential under microplastic stress, (ii) examine the reactions of soil microorganism communities to the combined treatment, and (iii) evaluate the potential of this biochar-phosphate fertilizer combined approach to enhance soybean growth and phosphorus utilization efficiency. This research not only advances our understanding of the interactions between biochar, phosphate fertilizer, and microplastics in agricultural systems but also provides valuable theoretical and practical insights for developing sustainable soil management strategies in the context of increased microplastic pollution and global phosphorus resource constraints. The findings are expected to contribute to promoting the application of biochar and phosphate fertilizer joint technology, offering a potential approach to maintaining soil health and crop productivity in contaminated environments.

2. Materials and methods

2.1. Experimental soil, LDPE-MPs, and maize-derived biochar

Experimental soil (0–30 cm in depth) was collected from the Environmental Research Base of Liaocheng University, Shandong Province, China (116°00′29″ E, 36°25′43″ N). The sampling site was neither overlaid with plastic mulch nor contaminated by pollutants. To preserve the microbial community characteristics, the soil samples were air-dried at room temperature and then sieved using a 2-mm sieve to eliminate debris. After thorough mixing, the soil was stored at 4℃ until further use. LDPE microplastics with a diameter of 150 μm and a density of 0.95 g/cm^3 were provided by Huachuang Plastics Co., Ltd. (Guangdong, China). Biochar, obtained from Zhironglian Technology Co., Ltd. (Nanjing, China), was fabricated by pyrolyzing corn straw at 500 °C in a controlled-atmosphere furnace. Its preparation and attributes are detailed in Text S1 and Table S1. Additionally, scanning electron microscopy (SEM) indicated that the biochar surface is rough, with a large number of irregularly shaped pore structures; some of these pores show signs of structural collapse, and the surface is additionally covered with a significant amount of particulate matter (Fig. S1 and Text S2). Fourier transform infrared (FTIR) revealed characteristic absorption peaks at 1066.5 cm^{-1} , 1402.5 cm^{-1} , 1601.2 cm^{-1} , and 3134.9 cm^{-1} (Fig. S2 and Text S2).

2.2. Soybean potting experiment setup

The pot experiment, designed with biochar level as the primary factor and P fertilization level as the secondary factor, was undertaken in June 2023 at the Environmental Research Base of Liaocheng University (Shandong Province, China) to investigate the synergistic improvement effects of both on microplastic-polluted soil. Located in a typical temperate monsoon climate, the experimental site experiences an average annual temperature of 13.6°C and an average annual precipitation of 550 mm. Phosphate was applied in the form of KH_2PO_4 at rates of 0, 30, 60, 90, and 180 kg P ha^{-1}, either as standalone treatments (designated as P0, P30, P60, P90, and P180) or in combination with 2 % biochar (w/w) (designated as B-P0, B-P30, B-P60, B-P90, and B-P180, respectively). All treatments were replicated three times (n = 3, N = 30). Target-concentration pristine microplastics (1 %, w/w) were blended with 24 kg of air-dried, sieved soil per pot in a stainless-steel basin. The mixture was stirred continuously with a clean glass rod for 30 min, followed by one week of pre-equilibration. Then, this composite was thoroughly mixed with biochar and phosphorus fertilizer (at treatment-specific ratios) by the same method, ensuring no obvious agglomeration of individual materials. Homogeneous mixtures were transferred into pots (height = 23 cm, length = 36 cm), which were placed into holes in an experimental field such that each pot's top was flush with the soil surface. 2 L of water was poured into each pot prior to the initiation of the trial. Additionally, each treatment received a one-time application of 48 kg ha^{-1} urea as a base fertilizer. Subsequently, each pot was planted with three soybean seedlings (Zhonghuang 13, obtained from Jining Shengyuan Seed Industry Co., Ltd.) at a depth of 3 cm. Regular irrigation

was provided to ensure normal plant growth, keeping the amount of irrigation uniform across all treatments. Upon reaching maturity, soybean plants were harvested from each pot. After carefully removing loosely adhering soil, the soil firmly attached to the roots was collected as rhizospheric soil, whereas the remaining soil was classified as bulk soil. The collected soil samples were split into two subsamples: one was stored at 4°C for analysis of soil physicochemical characteristics, while the other was preserved at −20°C for soil microbiome analysis.

A concentration of 1 % (w/w) MPs was used because its environmental concentration in polluted soil is commonly in the range of 0.0–1 % and 1 % MPs are usually employed in previous studies (Zhang et al., 2024). A 2 % biochar application rate was selected since it can promote soil nutrient cycling and alleviate microplastic stress (Zhao et al., 2025), and is also consistent with practical application levels (Harter et al., 2013). Phosphate levels of 30–90 kg ha^{-1} were selected to reflect typical P fertilization rates in China (Tian et al., 2021), while 180 kg P ha^{-1} was included to assess the exaggerated effects of high phosphate levels on the soil ecosystem. Based on prior research, P treatments were categorized as follows: 0 and 30 kg P ha^{-1} were defined as low-concentration treatments, 60 and 90 kg P ha^{-1} as medium-concentration treatments, and 180 kg P ha^{-1} as the high-concentration treatment (Fink et al., 2020; Tian et al., 2021).

2.3. Plant samples analysis

Soybean plants were separated into roots, stems, leaves, kernels, and pods. Notably, the roots were thoroughly rinsed with tap water, followed by ultrapure water, and then placed on clean filter paper to absorb moisture before subsequent analysis. Plant samples were dried in an oven at 65°C until a constant weight was achieved, then cooled to room temperature in a desiccator for dry weight measurement. The phosphorus concentration in the soybeans was ascertained using the vanadium-molybdenum yellow spectrophotometric method. Detailed experimental procedures are outlined in Text S3.

2.4. Soil physicochemical characteristics analysis

Soil pH was determined using a pH electrode (PHS-3C, Leici, Shanghai, China) at a soil-to-water ratio of 1:5 (w/v). NO_3^--N and NH_4^+-N concentrations were quantified via UV spectrophotometry (U-2900, Hitachi, Tokyo, Japan) according to dual-wavelength UV spectrophotometry and indophenol blue spectrophotometry, respectively (HJ 634–2012). Total nitrogen (TN) content was analyzed by an elemental analyzer (Vario MICRO cube, Elementar, Germany). Soil total phosphorus (TP) was measured by the alkali fusion-Mo-Sb spectrophotometric method (HJ 632–2011). The TOC analyzer (Shimadzu TOC-Vcph, Japan) was employed to ascertain soil dissolved organic carbon (DOC) and total carbon (TC). Available phosphorus (AP) concentration in the supernatant was quantified by spectrophotometry after soil retrieval with 0.5 mol/L $NaHCO_3$ (HJ 704–2014). Soil physicochemical assays used two technical replicates per biological replicate (three biological replicates; one pot = one biological replicate).

2.5. Microbial community analysis

Three topsoil samples per pot were collected, mixed into a composite sample, and then freeze-dried for 48 h for subsequent experiments. Following instructions provided by the manufacturer, DNA was retrieved from 0.5 g of lyophilized soil using the FastDNA SPIN Kit (MP Biomedicals, Germany). DNA quality was appraised with a NanoDrop ND-1000 spectrophotometer (NanoDrop Technologies, Inc.). The abundance of 16S rRNA, 18S rRNA, and *phoD* genes was quantified using a Roche LightCycler 96, with three technical replicates per biological replicate. Details of the primers and cycling conditions are presented in Table S2. Purified amplicons, pooled in equimolar concentrations, were sequenced (2 ×250 bp) on the Illumina NovaSeq platform using the NovaSeq 6000 SP Reagent Kit (500 cycles) by Shanghai Personal Biotechnology, Ltd. (Shanghai, China), with one technical replicate per biological replicate.

2.6. Statistical analysis

The distinctions in various indicators of rhizosphere and bulk soils across different treatments were analyzed using SPSS (version 25, IBM, Inc., United States) and Excel (version 2021, Microsoft, Inc., United States). For data meeting normality and variance homogeneity assumptions, one-way analysis of variance (ANOVA) followed by the least significant difference method (LSD) was performed. For data violating these assumptions, the non-parametric Kruskal-Wallis test was used to determine significant variations among treatments. Principal coordinate analysis (PCoA) based on Bray-Curtis dissimilarity was employed to investigate variations in environmental factors between rhizosphere and bulk soils across different treatments. The influences of phosphorus fertilizer, biochar, and their interaction on soybean biomass, phosphorus content, phosphorus uptake, and yield were evaluated using two-way analysis of variance (two-way ANOVA). The microbial community data were Hellinger-transformed to downweight highly abundant taxa and reduce heteroscedasticity; subsequently, non-metric variations in fungal community beta-diversity among treatments were examined using Multidimensional Scaling (NMDS) and permutational multivariate analysis of variance (PERMANOVA). Redundancy analysis (RDA) was performed to probe connections between soil characteristics and fungal community composition. Microbial co-occurrence network analysis was carried out with R software (version 4.3.1) and Gephi (version 0.9.3) to assess associations among microbial taxa. To further elucidate the multivariate associations between functional genes and parameters, this study performed the Mantel test. Additionally, partial least squares path modeling (PLS-PM) was implemented using the R package "*plspm*" to comprehensively capture the latent effects of biochar, phosphate fertilizer, soil physicochemical factors, functional gene abundance, and fungal community diversity on soybean phosphorus uptake and yield.

3. Results

3.1. Effects of biochar–fertilizer integration on soil physicochemical properties

Bulk and rhizospheric soils exhibited considerable differences in physicochemical properties, as demonstrated by PCoA (Fig. 1). To be specific, there were interpretation rates of 83.64 % and 12.08 % for the first and second axes, respectively. Treatments with and without biochar in rhizospheric soil displayed a dispersed distribution, suggesting that biochar significantly influenced its physicochemical properties. In contrast, bulk soil showed clustering, indicating a lesser impact of biochar. Overall, biochar altered soil physicochemical characteristics, with a more pronounced impact on rhizospheric soil.

Incorporation of biochar at different phosphorus fertilizer levels induced pronounced differences in soil physicochemical properties (Table S3). Introducing phosphorus fertilizer without biochar input notably reduced the pH of the rhizosphere soil ($P < 0.05$), whereas no notable effect was detected in the bulk soil. Moreover, the mean pH value in rhizosphere soil (7.87) was considerably lower than that in the bulk soil (8.00) ($P < 0.05$). Biochar supplementation at medium P fertilizer levels (B-P60, B-P90) significantly decreased NH_4^+-N content ($P < 0.05$) in rhizosphere and bulk soils. Additionally, NO_3^--N and TN contents were notably diminished under the P90 treatment compared with the B-P90 treatment in bulk soil ($P < 0.05$). Nevertheless, no remarkable variations were noted in rhizosphere soil. Furthermore, applying biochar significantly increased DOC content ($P < 0.05$) at 0, 30, and 60 kg P ha^{-1} levels (B-P0, B-P30, and B-P60), while no considerable variation was observed in the bulk soil. Interestingly, biochar–fertilizer integration considerably increased AP concentration

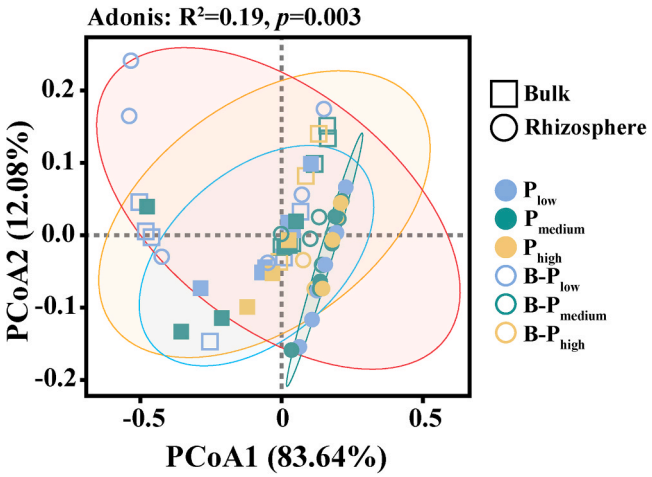

Fig. 1. Principal coordinate analysis (PCoA) of distinct samples based on the Bray-Curtis distance metric of soil physicochemical properties, divided into four confidence ellipses with colors indicating treatments: Red for rhizosphere soil with biochar; Green for rhizosphere soil without biochar; Orange for bulk soil with biochar; Blue for bulk soil without biochar. Notes: P_{low} indicates low phosphorus concentration (0 and 30 kg P ha^{-1}); P_{medium} indicates medium phosphorus concentration (60 and 90 kg P ha^{-1}); P_{high} indicates high phosphorus concentration (180 kg P ha^{-1}); B-P_{low}, B-P_{medium}, and B-P_{high} indicate the corresponding phosphate fertilizer level in combination with 2 % biochar.

relative to the B-P0 group in the rhizosphere soil, particularly in the B-P60 and B-P90 groups, with increases of 130.13 % and 135.19 %, respectively ($P < 0.05$). Nevertheless, the phenomenon mentioned above was not observed in the bulk soil. Compared with the P0 treatment, the B-P0 treatment markedly decreased TP concentration in bulk soil (71.8 %) and rhizosphere soil (80.0 %) ($P < 0.05$). However, phosphorus input after applying biochar raised the TP content. A key finding was that biochar increased TC concentration and the C/N ratio in the rhizosphere soil, peaking in the B-P60 treatment. In contrast, biochar had no remarkable impact on these parameters in bulk soil except in the B-P0 treatment. Moreover, the C/P ratio decreased remarkably with the input of P in biochar-treated groups in the rhizosphere ($P < 0.05$), while no significant divergences were found in the bulk soil apart from the P60 treatment. Similarly, the N/P ratio declined significantly when P-fertilizer was incorporated into the biochar-treated groups compared with the B-P0 treatment across both rhizosphere and bulk soils ($P < 0.05$).

3.2. Effects of biochar–fertilizer integration on soybean growth

The phosphorus content in soybean organs showed differential responses to various treatments (Fig. S3, Tables S4 and S5). Administering phosphate fertilizer alongside biochar remarkably increased phosphorus concentration in pods ($P < 0.05$) relative to B-P0 treatment, with the maximum content of 5.49 $mg{\cdot}g^{-1}$ observed in the B-P60 treatment (Fig. S3a, Tables S4 and S5). Compared with the P0 treatment, P30 and P60 treatments substantially increased phosphorus content in kernels by 39.4 % and 38.3 %, respectively ($P < 0.05$) (Fig. S3b, Tables S4 and S5). However, phosphate fertilizer implementation did not considerably alter phosphorus concentration in leaves (Fig. S3e, Tables S4 and S5). Under the same phosphate fertilizer levels, biochar addition did not considerably alter phosphorus concentrations in pods, kernels, and leaves. In contrast, biochar influenced P concentrations in stems and roots (Figs. S3c,d, Tables S4 and S5). Specifically, root phosphorus concentration in the B-P60 treatment was remarkably beyond that in P60 ($P < 0.05$), whereas the situation was opposite in the B-P180 (Fig. S3c, Tables S4 and S5). Similarly, stem phosphorus concentration in the P180 was distinctly greater in comparison to that of the B-P180 treatment ($P < 0.05$) (Fig. S3d, Tables S4 and S5).

Concurrent application of biochar and moderate phosphorus fertilizer levels (B-P60, B-P90) was advantageous for increasing soybean total biomass and yield in MPs-contaminated soil (Fig. 2, Tables S4 and S5). No notable differences were detected in biomass (including shoot, root, and total) and yield under single phosphorus fertilizer application. An intriguing observation was that biomass and yield increased initially and then declined as P-fertilizer input increased under biochar application (Fig. 2a-d, Tables S4 and S5). Extraordinarily, B-P60 and B-P90 treatments reached the optimal outcomes. In addition, biochar amendment did not notably affect biomass and yield. However, the total biomass in P30, P60, and P90 levels increased by 21.38 %, 40.73 %, and 42.58 % respectively after the addition of biochar (Fig. 2c, Tables S4 and S5). Analogously, soybean yield in B-P30, B-P60, and B-P90 treatments increased by 45.97 %, 74.38 %, and 84.16 % compared with that in P30, P60, and P90 treatments (Fig. 2d, Tables S4 and S5).

Multiplying phosphorus concentration by biomass was used to obtain the P uptake of the plant (mg P $plant^{-1}$). Results indicated that adding biochar under low and medium P input significantly increased phosphorus uptake in pods (Fig. S4a, Tables S4 and S6). Nevertheless, no such effect was observed for P uptake in other plant parts (Figs. S4b-e, Tables S4 and S6). In addition, the total phosphorus uptake in P30, P60 and P90 levels increased by 42.69 %, 58.19 % and 34.44 %, respectively after the addition of biochar (Fig. S4f, Tables S4 and S6).

3.3. Effects of biochar–fertilizer integration on functional gene abundance

Quantitative PCR results revealed that biochar amendment affected the abundance of the *phoD*, 16S rRNA, and 18S rRNA genes in MPs-contaminated alkaline soil (Fig. 3). Specifically, the *phoD* gene copy numbers in B-P0, B-P30, and B-P60 treatments were substantially greater than those in bulk soil of P0, P30, and P60 treatments ($P < 0.05$) (Fig. 3a). In rhizospheric soil, incorporating biochar notably enhanced the prevalence of the *phoD* gene at the P30 and P60 input levels ($P < 0.05$), while the opposite trend was observed at the P90 level (Fig. 3d). Interestingly, 16S rRNA gene abundance was noticeably higher in the B-P30, B-P60, and B-P90 treatments relative to the P30, P60, and P90 treatments in bulk soil ($P < 0.05$) (Fig. 3b). Nevertheless, biochar did not notably alter 16S rRNA gene abundance in rhizospheric soil (Fig. 3e). In addition, 18S rRNA gene abundance was remarkably increased in the B-P30 and B-P60 treatments compared with the corresponding treatments without biochar addition in bulk soil ($P < 0.05$), with a comparable trend perceived in rhizospheric soil (Fig. 3c,f).

3.4. Effects of biochar–fertilizer integration on fungal community

Changes in the α-diversity of fungal microbiota in both bulk soil and rhizospheric soil under various treatments were evaluated using Illumina MiSeq sequencing technology (Table S7). In the bulk soil, biochar did not considerably alter the ACE metrics. Nevertheless, the fungal community had lower Pielou and Shannon indices in the B-P30 treatment than the P30 treatment, while the Simpson index showed a reverse trend ($P < 0.05$). In rhizosphere soil, biochar did not notably impact the Shannon and Simpson metrics, but the ACE richness index was remarkably higher in the B-P30 group compared with the P30 group ($P < 0.05$). Moreover, B-P90 treatment had a lower Pielou index relative to P90 treatment ($P < 0.05$).

Administering biochar did not uniformly affect the amount of fungal OTUs (Fig. S5). A total of 269 and 274 common fungal OTUs were detected in bulk soil and rhizospheric soil samples, respectively. In bulk soil, the highest number of specific genera (94) was detected in the P60 treatment, whereas the lowest (54) was found in the B-P30 treatment (Fig. S5a). In rhizosphere soil, the highest (333) and lowest (52) numbers of specific genera were observed in the B-P30 and B-P60 treatments, respectively (Fig. S5b). Further, the variations in fungal community composition at the genus level in bulk and rhizospheric soils were investigated (Fig. 4a,b). In bulk soil, the top ten dominant genera

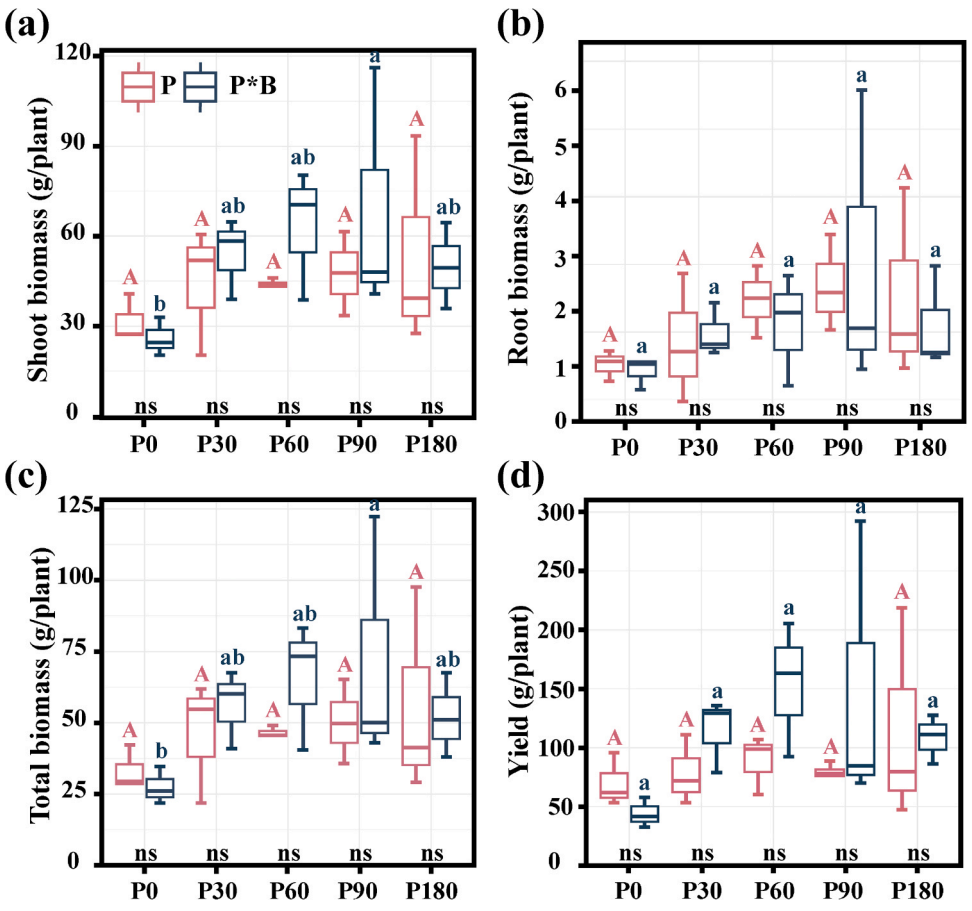

Fig. 2. Effects of different treatments on shoot biomass (a), root biomass (b), total biomass (c), and yield (d). Uppercase letters indicate the differences among biochar-unsupplemented treatments, and lowercase letters indicate differences among treatments under biochar supplementation ($p < 0.05$). Significant differences among treatments with or without biochar at the same phosphate fertilizer level are indicated as follows: *$p < 0.05$, **$p < 0.01$, ***$p < 0.001$. "ns" represents situations where no statistically significant differences exist. P0, P30, P60, P90, and P180 signify P input at 0, 30, 60, 90, and 180 kg P ha^{-1}, respectively. "P": only phosphate fertilizer; "P*B": phosphate fertilizer with 2 % biochar (mean ± SD, n = 3).

included *Unassigned* (20.01 %-37.97 %), *Fusarium* (9.92 %-42.97 %), *Ascobolus* (1.87 %-17.69 %), *Verticillium* (2.29 %-9.31 %), *Mortierella* (3.34 %-9.46 %), *Chaetomium* (0.47 %-4.48 %), *Humicola* (0.69 %-2.66 %), *Plectosphaerella* (1.00 %-5.16 %), *Pseudallescheria* (0.19 %-8.41 %), and *Alternaria* (0.92 %-8.68 %). Meanwhile, it was shown that biochar notably augmented the relative prevalence of *Fusarium*, but decreased the relative prevalence of *Ascobolus* (Fig. 4a). In rhizospheric soil, the top ten dominant genera were *Unassigned* (15.21 %-30.41 %), *Verticillium* (1.5 %-25.81 %), *Fusarium* (25.76 %-44.21 %), *Mortierella* (2.01 %-6.29 %), *Ascobolus* (0.39 %-17.61 %), *Aspergillus* (0.35 %-5.56 %), *Alternaria* (0.40 %-5.15 %), *Chaetomium* (0.63 %-4.09 %), *Humicola* (0.31 %-3.30 %), and *Plectosphaerella* (0.72 %-5.79 %). Analysis showed that after incorporating biochar, the abundances of *Fusarium* and *Verticillium* were strikingly increased, while the prevalence of *Ascobolus* was conspicuously decreased. Furthermore, the B-P60 and B-P90 groups increased the relative prevalences of *Fusarium* and *Aspergillus*, respectively, compared to their non-biochar counterparts (Fig. 4b). Notably, *Fusarium* species can generate various organic acids to solvate phosphorus (Marcos et al., 2023). Similarly, *Aspergillus* facilitates the release and dissolution of phosphorus through producing metabolites and secreting organic acids (Fu et al., 2024).

The differences in network metrics can reflect the complexity and diversity of fungal community structure and function (Fig. 4c-f). The quantity of positive associations was higher than the number of negative ones in rhizospheric and bulk soils (Fig. 4c,d). Additionally, the rhizosphere soil network (Nodes=181, Edges=190) was more complicated than that of bulk soil (Nodes=94, Edges=85). Notably, in rhizospheric soil, biochar addition notably increased the quantity of nodes and edges compared to non-biochar treatments (Fig. 4e,f). These results suggest that microbial interactions and network complexity follow the order: rhizosphere soil > bulk soil, and with biochar > without biochar.

NMDS and PERMANOVA unveiled variations in fungal communities among treatments in both bulk and rhizospheric soils (Fig. 5a,b). Fungal communities with and without biochar addition showed a dispersed distribution in bulk soil (R^2=0.098) and rhizosphere soil (R^2=0.085), indicating that biochar significantly influenced community structures. In contrast, fungal communities aggregated based on P input levels in bulk soil (R^2=0.134) and rhizosphere soil (R^2=0.128), suggesting that phosphate fertilizer had no significant impact on community structures. Therefore, we inferred that biochar, rather than phosphate fertilizer, caused marked changes in the fungal communities.

3.5. Comprehensive effects of biochar–fertilizer integration on soybean-soil system

RDA was employed to evaluate the effects of soil physicochemical attributes on fungal communities in bulk and rhizosphere soils (Fig. 5c, d). In bulk soil, all environmental elements accounted for 14.09 % of the variation, in which Axis 1 and Axis 2 contributed 8.23 % and 5.86 %, respectively. TN (R^2=0.30; $P = 0.045$), N/P ratio (R^2=0.48; $P = 0.003$) and C/P ratio (R^2=0.34; $P = 0.009$) were the primary factors influencing fungal community composition (Fig. 5c). In rhizosphere soil, all environmental elements accounted for 17.06 % of the variation, in which Axis 1 and Axis 2 contributed 9.0 % and 8.06 %, respectively. DOC

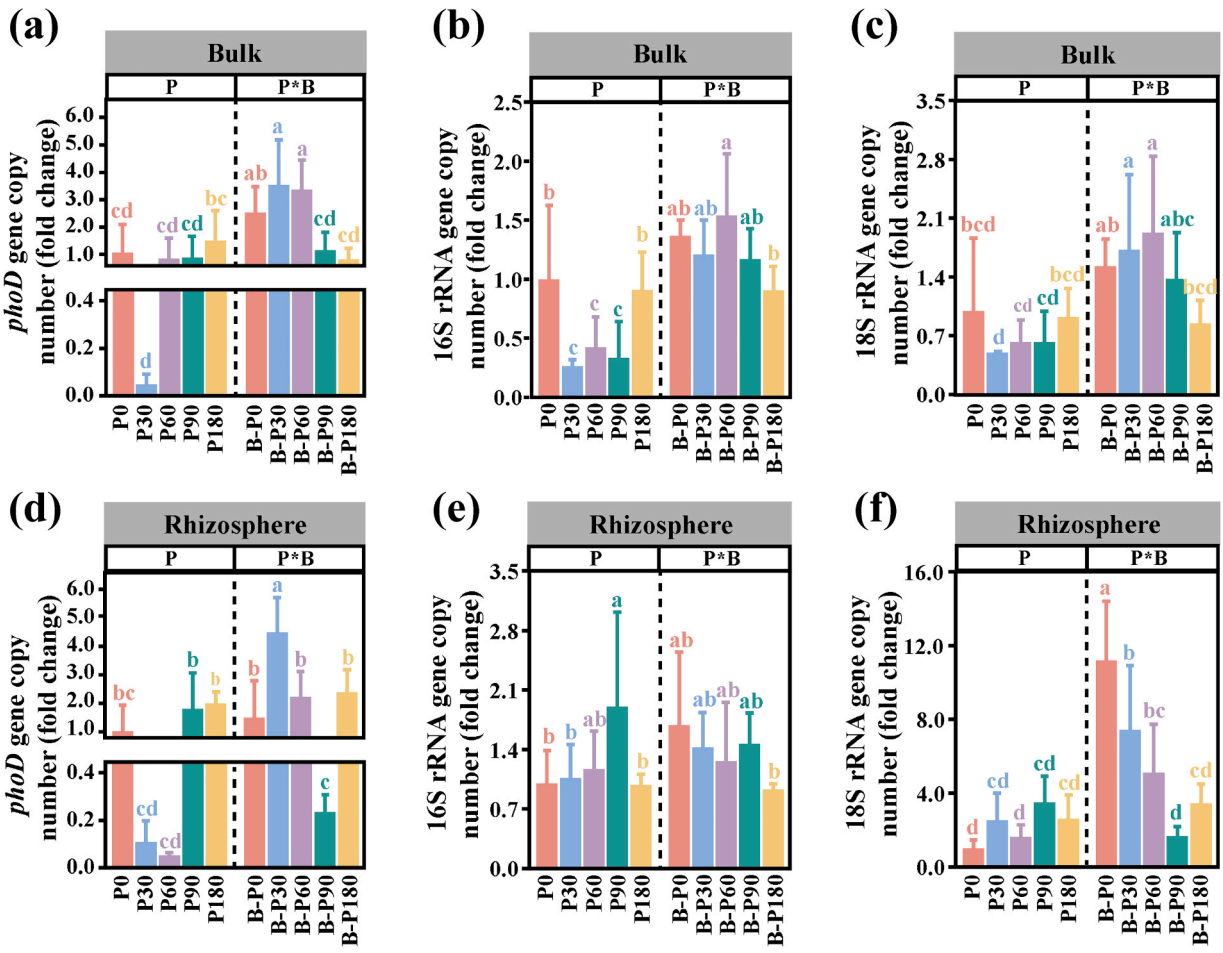

Fig. 3. Copy numbers of soil microbial functional genes related to phosphorus conversion (*phoD*) (a,d), bacteria (16S rRNA) (b,e), and fungi (18S rRNA) (c,f) in bulk and rhizosphere soils under various treatments. The lowercase letters indicate differences among treatments ($p < 0.05$). P0, P30, P60, P90, and P180 indicate P fertilizer applied at 0, 30, 60, 90, and 180 kg P ha^{-1}, respectively; "P": only phosphate fertilizer; "P*B": phosphate fertilizer with 2 % biochar (mean ± SD, n = 3).

(R^2=0.21; $P = 0.039$), TN (R^2=0.46; $P = 0.001$), AP (R^2=0.28; $P = 0.02$), TC (R^2=0.34; $P = 0.005$) and C/N (R^2=0.33; $P = 0.05$) were the key parameters shaping fungal community composition (Fig. 5d).

To further explore the connections between soil parameters and the microbiome, mantel tests were performed to analyze the correlations across the abundances of *phoD*, 16S rRNA and 18S rRNA genes and soil parameters in bulk and rhizosphere soils (Fig. 5e). Mantel test results revealed that in bulk soil, *phoD* gene abundance manifested a pronounced positive connection with DOC content. The 16S rRNA gene abundance exhibited a notable positive correlation with C/N ratio, while 18S rRNA gene abundance was actively correlated with TC, C/N ratio, and N/P ratio. In rhizosphere soil, only 18S rRNA gene abundance exhibited significant relationships with DOC, TP, AP, C/P ratio, and N/P ratio, whereas *phoD* and 16S rRNA gene abundances showed no significant correlations with soil physicochemical parameters.

PLS-PM was constructed to capture the intrinsic interactions among soil fungi, soil physicochemical parameters and plant growth (Fig. 6). The results revealed that biochar application exerted a positive impact on fungal diversity in bulk soil (Fig. 6a) ($P < 0.001$), but a direct negative influence in rhizosphere soil (Fig. 6b) ($P < 0.01$). Similarly, P input exerted direct positive and adverse effects on the physicochemical parameters of both bulk soil and rhizosphere soil, with path coefficients of 0.7 ($P < 0.001$) and 0.35 ($P < 0.05$), respectively. Additionally, biochar application significantly improved the physicochemical parameters of rhizospheric soil. An interesting finding was that soil physicochemical properties directly influenced fungal diversity and gene abundance in the rhizosphere soil, with path coefficients of 0.59 ($P < 0.05$) and 0.69 ($P < 0.001$), respectively (Fig. 6b). This phenomenon was not observed in bulk soil. Both biochar and phosphate fertilizer directly or indirectly affected plant phosphorus uptake, ultimately influencing soybean yield. Significantly, biochar exerted a notable direct influence on the rhizosphere ($P < 0.001$) as well as the bulk areas ($P < 0.05$), and the rhizosphere zone showed a more pronounced response (Fig. 6c). Meanwhile, changes in rhizospheric soil exerted a positive role in promoting the phosphorus uptake of soybeans, thereby indirectly increasing soybean yields.

4. Discussion

4.1. Mechanisms underlying fungal community responses to biochar-fertilizer integration

Fungi perform essential functions in soil ecosystems as decomposers and symbionts, significantly influencing nutrient mobilization and fixation, while they are generally interconnected through complex ecological interaction networks rather than existing in isolation (Zhang et al., 2022). Differentiation in co-occurrence networks suggested that biochar application increased the negative links among microbial populations in the rhizosphere soil (Fig. 4e, f). This implies that the fungal communities exhibited a greater number of competitive associations. Plenty of organic substances were provided by biochar, which promoted microbial activity and generated additional metabolites that suppressed the activity of other microorganisms, thus intensifying competition among them (Yan et al., 2021). Furthermore, there were more nodes and

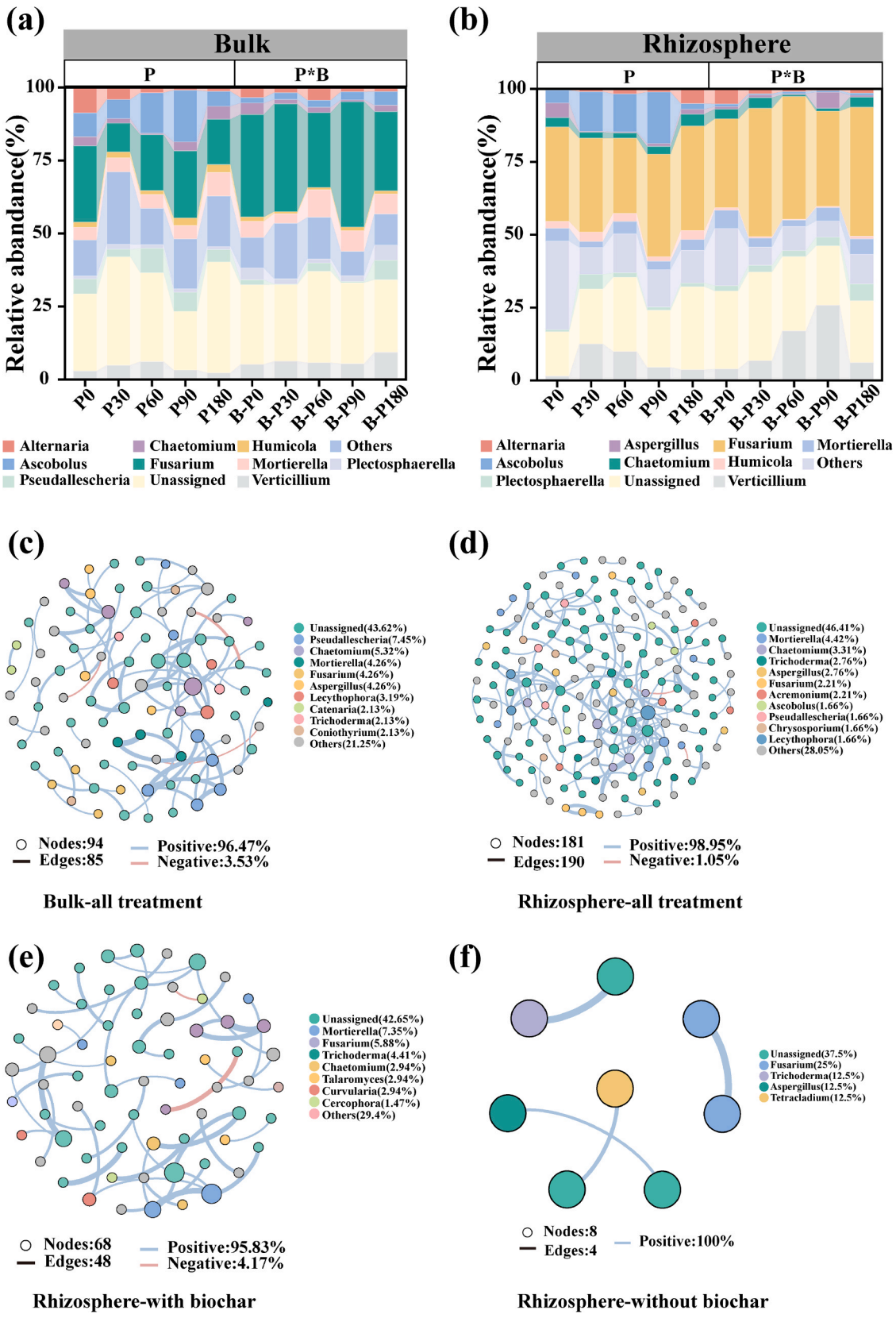

Fig. 4. Relative prevalence of fungal microbial community at genus level in bulk soil (a) and rhizosphere soil (b). Co-occurrence networks of fungal communities in bulk soil (c), rhizosphere soil (d), and rhizosphere soil with (e) or without (f) biochar treatments. The size of each node represents the relative abundance of OTUs within the fungal microbial communities under the treatments. A blue edge indicates a significantly positive relationship, while a red edge demonstrates a significantly negative relationship between two individuals. P0, P30, P60, P90, and P180 demonstrate P fertilizer applied at 0, 30, 60, 90, and 180 kg P ha^{-1}, respectively; "P": only phosphate fertilizer; "P*B": phosphate fertilizer with 2 % biochar.

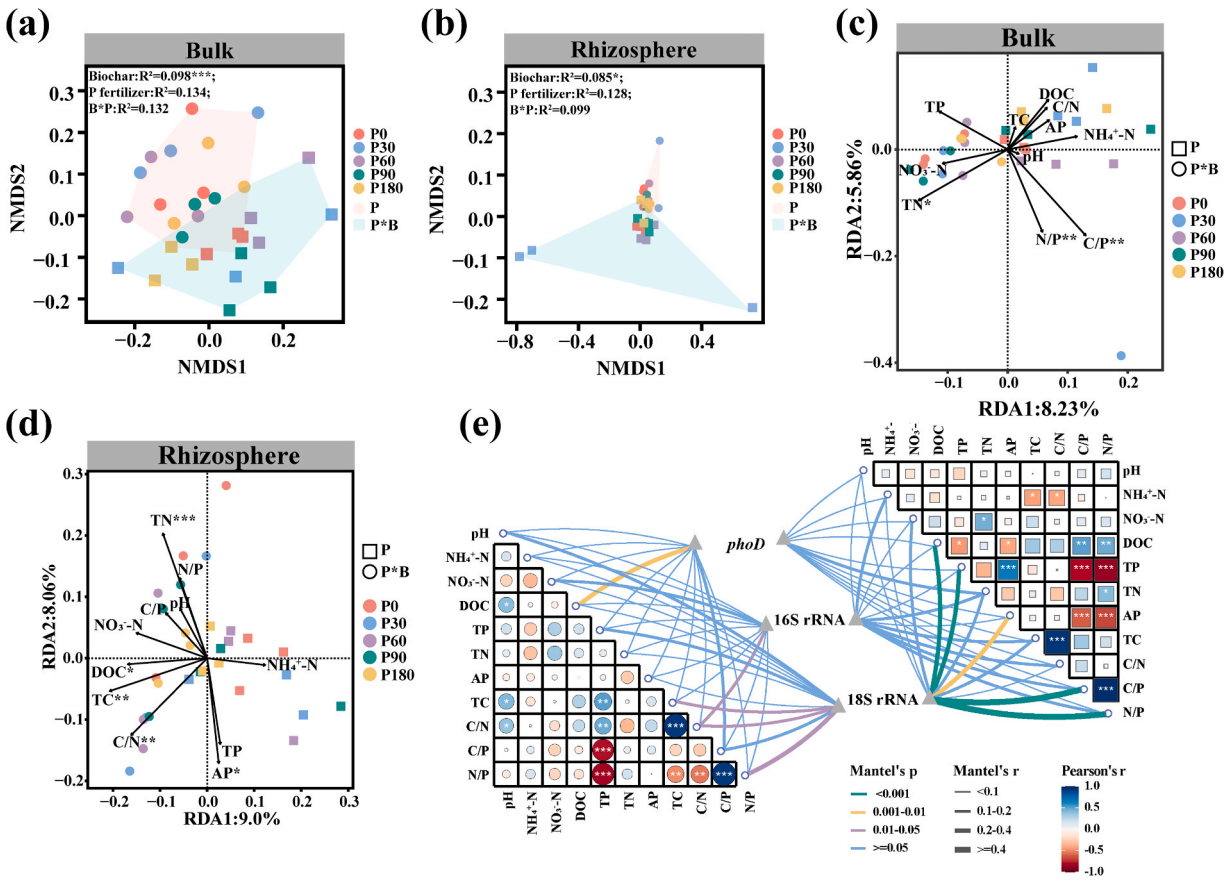

Fig. 5. NMDS and PERMANOVA reveal variations in fungal community composition between bulk soil (a) and rhizosphere soil (b) under different treatments. RDA assesses the relationship between fungal community composition and soil characteristics in bulk soil (c) and rhizosphere soil (d). The figure illustrates the Pearson correlation coefficients assessing the associations between genes and soil physicochemical characteristics in bulk soil (Lower triangle) and rhizosphere soil (Upper triangle) (e). Edge color represents the statistical significance (green: $p < 0.001$, orange: $p = 0.001$–0.01, purple: $p = 0.01$–0.05, blue: $p > = 0.05$) and edge width corresponds to the Mantel's r statistic for the corresponding distance correlations. P0, P30, P60, P90, and P180 indicate P fertilizer applied at 0, 30, 60, 90, and 180 kg P ha^{-1}, respectively; "P": only phosphate fertilizer; "P*B": phosphate fertilizer with 2 % biochar.

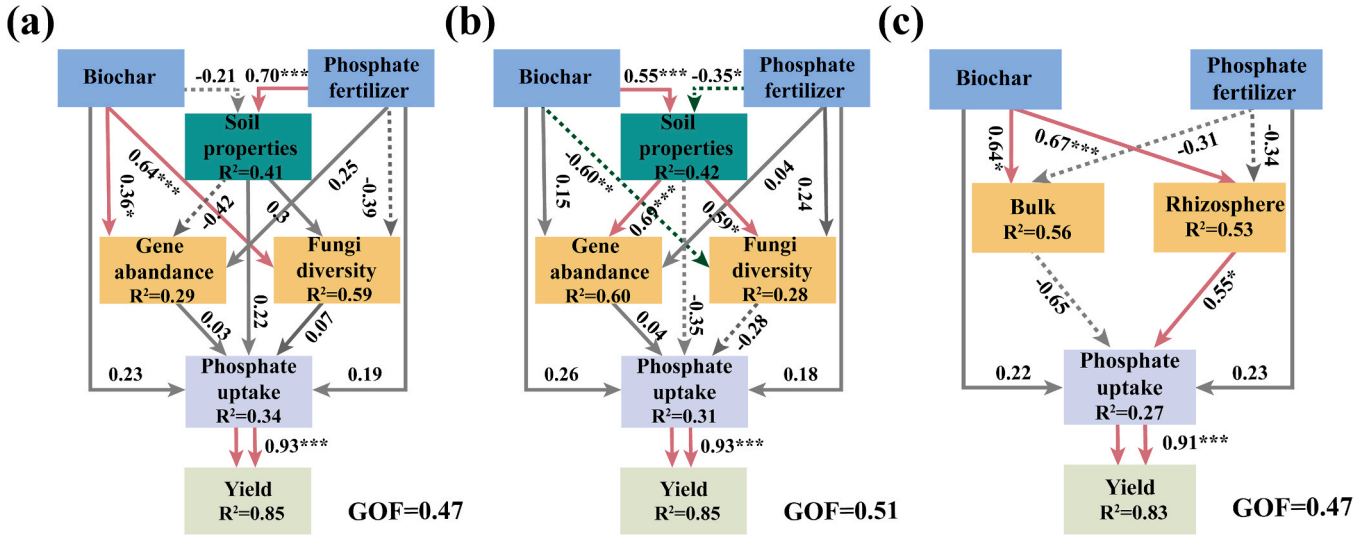

Fig. 6. PLS-PM analysis depicting potential relationships among biochar, phosphate fertilizer, fungal communities, soil properties, phosphate uptake, and yield in bulk soil (a) and rhizosphere soil (b). Impacts of biochar, phosphate fertilizer, bulk soil, and rhizosphere soil on yield (c). Positive and negative effects are denoted by solid and dashed lines, respectively.

connections in the microbial networks of rhizospheric soil than in those of bulk soil, signifying high complexity and stability within microbial communities, and complex networks can generally support more diverse ecosystem service functions (Fig. 4c, d). This may result from the rhizosphere providing greater possibilities for niche sharing and interactions among microorganisms (Zhu et al., 2023).

The results accentuated that biochar application profoundly altered the fungal community structure and composition in microplastic-contaminated alkaline soils (Fig. 5a, b). These changes can be attributed to several mechanisms. First, biochar modifies root exudates of soybean, selectively favoring specific microbial populations and thereby reshaping the microbial community structure (Wu et al., 2015). Second, the porous surface configuration of biochar alongside functional groups (-OH, C-O, and C═O) (Text S2, Figs. S1 and S2) can augment the adsorption of MPs by expediting hydrogen bonding with them or forging complexes, mitigating impacts on fungal communities (Ji et al., 2024). Third, transformations in community abundance and structure can be directly or indirectly driven by variations in soil microenvironment (including pH value, nutrient availability, and organic matter dynamics) caused by biochar utilization (Figs. 1, 6, and Table S3), which is consistent with previous results (Cha et al., 2021). Further, we discovered that fungal microbiota diversity and functional gene abundance were more closely correlated with physicochemical properties of rhizospheric soil according to PLS (Fig. 6b, c), indicating that alterations in rhizospheric soil nutrients directly contributed to transformation in microbial diversity (Liu et al., 2020). Zhu et al. (2023) also indicated that microbiota were responsive to the rhizosphere effects, saline-alkalinity, and organic carbon composition.

An intriguing observation was that co-application of biochar and appropriate phosphate fertilizer enriched specific functional microorganisms, thereby enhancing the bioavailability of nutrients such as carbon and phosphorus (Fig. 4a, b). For instance, *Aspergillus* can release phosphorus from Fe-P and Ca-P by secreting citric acid and oxalic acid and produce enzymes and metabolites to accelerate phosphate dissolution (Fu et al., 2024). *Fusarium* is known to mobilize phosphorus and facilitate its release from mineral complexes by producing organic acids (Marcos et al., 2023). Xu et al. (2018) validated the hypothesis that fungal communities were modulated by soil P availability, where both insufficient and excessive available phosphorus hindered fungal growth and development. Phosphorus is the principal nutrient constraint on microbial metabolism, and microbial groups capable of solubilizing P tend to dominate under P-deficient conditions (higher C/P and N/P ratios) (Ning et al., 2021). However, our results showed that introducing biochar alone markedly increased soil C/P and N/P ratios($P < 0.05$), while its combined application with phosphate fertilizer significantly decreased these ratios ($P < 0.05$), particularly in rhizosphere soil (Table S3). This may be attributed to the rhizosphere effect, which elevates soil fertility and nutrient bioavailability, in turn furnishing a favorable habitat for fungal proliferation (Lu et al., 2024). And alleviating the discrepancy in the C/P ratio can accelerate microbial biomass P turnover and increase the release of P (Ning et al., 2021). Moreover, fungal communities can also utilize their hyphal networks to colonize biochar particles and macropores, and have the potential to derive nutrients and residual pyrolysis compounds from biochar (Mitchell et al., 2016). Additionally, the presence of MPs further complicates microbial dynamics. MPs can significantly increase the relative abundance of nitrogen-sequestering and P-solubilizing microorganisms, potentially altering nutrient cycling processes (Aralappanavar et al., 2024). This highlights the importance of accounting for the collective influence of biochar, phosphate fertilizer, and MPs on soil microbiota and nutrient dynamics.

4.2. Mechanisms of biochar-fertilizer integration on soybean growth and nutrient dynamics

Biochar, rich in carbon, phosphorus and potassium, and characterized by unique surface properties, is fundamental for improving soil fertility and supporting plant growth (Wang et al., 2024). The impact of biochar on plant phosphorus uptake remains controversial. Some studies suggest that biochar can enhance P acquisition by plants and amplify their growth (Tian et al., 2021). Conversely, other studies have reported that biochar reduces phosphorus uptake by plants (Zwetsloot et al., 2016). Soil type, biochar feedstocks, or application rate may explain this discrepancy, and variations in these factors potentially impact the results. In our study, biochar had no marked impact on the overall soybean P uptake. However, total phosphorus uptake in soybeans increased in the B-P60 and B-P90 treatments (Fig. S4f). This could result from *Aspergillus* and *Fusarium* enhancing phosphorus bioavailability by activating sedimentary phosphate (Prabhu et al., 2018). Meanwhile, *Aspergillus* and *Fusarium*, equipped with mycelia that exhibit robust adhesion to polyethylene (PE), decompose PE by deforming and damaging its morphology through exerting pressure or eliciting oxidation, thus mitigating the detrimental effects (Spina et al., 2021). Furthermore, biochar exhibits superior performance in adsorbing PE owing to its large surface area and porous structure (Fig. S1 and Text S2), thus reducing PE bioavailability and mitigating its adverse effects on the root system (Liu et al., 2025). Biochar amendments inhibit the adsorption or precipitation of phosphorus by metal cations such as Al^{3+}, Fe^{3+}, and Ca^{2+} after fertilization (Hong and Lu, 2018). Phosphorus fertilizer not only directly delivers phosphorus, but also boosts rhizosphere acidification and mobilizes recalcitrant P, which may facilitate soybean growth and P uptake (Tian et al., 2022). Moreover, legumes can facilitate phosphorus and micronutrients by acidifying the rhizosphere or complexing with cations such as Fe^{3+} or Al^{3+} on soil mineral surfaces (Lu et al., 2024). Under high-P input (180 kg P ha^{-1}), soil available phosphorus may exceed the critical level required for optimal crop productivity, diminishing the growth-promoting effects of phosphate fertilizer. Analogously, Wang et al. (2024) indicated that a moderate quantity of phosphorus fertilizer can improve crop yields, while excessive application results in diminishing returns. In addition, moderate nutrient intensity facilitated the amplification of rhizosphere effects for enhanced nutrient capture, while surplus phosphorus introduction in soils impaired root biological function and disrupted microbial phosphorus cycling (Zhang et al., 2023). In our experiment, it seems that medium phosphate fertilizer input with biochar amendment is more conducive to activating the phosphorus in microplastic-contaminated soil, thus promoting the growth of soybeans.

Biochar can mitigate continuous cropping obstacles and improve soybean growth and yield, which was covered in relevant research (Wu et al., 2022). Our research demonstrated that the inclusion of biochar increased soybean yield in alkaline soils polluted by MPs, though without statistical significance (Fig. 2d, Tables S4 and S5). One possible reason for the discrepancy is differences in soil properties. For instance, systematic reviews have shown that the positive effects of biochar on crop productivity are more noticeable in acidic soils, while its impact on alkaline soils is limited or negative (Tesfaye et al., 2021). These responses could be credited to the fact that alkaline soils exhibit stronger ammonia volatilization processes and Na toxicity effects, which reduce nutrient availability (particularly for phosphorus) (Gao et al., 2021). Adding alkaline biochar can increase soil alkalinity, thereby further exacerbating these negative effects. Notably, the synergistic application of phosphate fertilizer with biochar, especially in the B-P60 and B-P90 treatments, positively impacted the soybean growth and yield (Fig. 2c,d, Table S4 and S5). Ye et al. (2020) also observed that combining biochar with inorganic fertilizers improved crop yield, while using biochar by itself had no noticeable effect. It is likely that phosphate fertilizer input with biochar affects element cycling and facilitates the absorption of phosphorus by soybeans, thereby increasing the yield (Fig. 6).

The rhizosphere, as the region where soil and plants interact, is momentous for enhancing plant growth and sustaining soil health (Bandopadhyay et al., 2024). We found that rhizosphere soil manifested a more robust response to biochar compared with bulk soil, and its

promotion of phosphorus absorption indirectly improved yield (Fig. 6c). Lu et al. (2024) demonstrated that the rhizosphere priming effect was essential in facilitating the mobilization of soil macronutrients and their availability for plant absorption. In addition, rhizosphere microbiota modulated plant nutrient acquisition by producing or metabolizing plant hormones in the rhizosphere, thereby sustaining elevated nutrient availability under soil heterogeneity (Xu et al., 2025).

Our findings underscore the capacity of combining phosphate fertilizer and biochar to mitigate the detrimental effects of MPs pollution on soil health and agricultural productivity. By enhancing P bioavailability and facilitating the development of P-solubilizing microorganisms, biochar can improve the efficiency of nutrient utilization and reduce reliance on chemical fertilizers. However, the effectiveness of biochar varies with soil type and pH, highlighting the need for site-specific management strategies. The rhizosphere effect performs a key function in nutrient mobilization and microbial activity, particularly in MP-contaminated soils. The long-term consequences of phosphate fertilizer and biochar on soil microbial communities and nutrient cycling under different agricultural practices and environmental conditions should be further investigated in future research. Additionally, the interactions among MPs, biochar, phosphate fertilizer, and soil microbiota warrant intensive investigation to develop comprehensive strategies for sustainable soil management.

In conventional agricultural production, the overuse of phosphate fertilizers not only restricts their bioavailability but also contributes to the depletion of phosphate rock resources and environmental pollution. Meanwhile, microplastics are widely present and constitute potential threats in agricultural ecosystems. We focus on investigating the effects of simultaneous biochar and phosphate fertilizer application on soil physicochemical properties, the fungal community, and crop growth in response to these dual challenges. The findings provide new perspectives for optimizing agronomic practices and enhancing crop productivity, while also highlighting the significance of formulating region-specific strategies for sustainable agricultural development.

5. Conclusion

In conclusion, our study demonstrates that biochar application in MPs-contaminated alkaline soils significantly alters fungal community structure and enhances P bioavailability, especially with medium-level P input. The integrated use of biochar and phosphate fertilizer stimulates the growth of phosphorus-solubilizing microorganisms, improves soybean phosphorus uptake, and increases yields. These findings further highlight biochar as a sustainable soil modification, effectively alleviating the adverse effects of microplastic contamination and boosting nutrient use efficiency in agricultural systems. Nevertheless, optimizing biochar application strategies demands considering soil type, initial nutrient content, and microplastic contamination levels as they influence the interaction between biochar and the soil environment. Additionally, long-term studies are required to gain insight into biochar's lasting effects on soil health, including physical and chemical properties, and on sustained crop productivity. In short, although our findings are promising, more work is required to fully harness these strategies for sustainable agriculture.

CRediT authorship contribution statement

Min Sun: Writing – original draft, Visualization, Methodology, Investigation, Conceptualization. **Xiao-Yu Li:** Methodology, Investigation, Formal analysis. **Hai-Yan Yuan:** Writing – review & editing, Supervision, Methodology, Conceptualization. **Qi-Lu Zhuang:** Methodology, Investigation. **Huan-Guang Deng:** Writing – review & editing, Supervision. **Bao-Xian Tao:** Writing – review & editing, Supervision. **Bao-Hua Zhang:** Writing – review & editing, Supervision.

Declaration of Competing Interest

The authors declare that they have no known competing financial interests or personal relationships that could have appeared to influence the work reported in this paper.

Acknowledgments

This subject was supported by the National Natural Science Foundation of China (grant number 42007219); the Doctoral Scientific Research Foundation of Liaocheng University (grant number 318052034) and the Students' Innovation and Entrepreneurship Training Program of Liaocheng University (grant number CXCY2023044).

Appendix A. Supporting information

Supplementary data associated with this article can be found in the online version at doi:10.1016/j.ecoenv.2025.119287.

Data availability

Sequencing data are available in the NCBI BioProject repository (ID: PRJNA1122412).

References

Aralappanavar, V.K., Mukhopadhyay, R., Yu, Y.X., et al., 2024. Effects of microplastics on soil microorganisms and microbial functions in nutrients and carbon cycling-A review. Sci. Total Environ. 924, 171435. https://doi.org/10.1016/j.scitotenv.2024.171435.

Bandopadhyay, S., Li, X., Bowsher, A.W., et al., 2024. Disentangling plant- and environment-mediated drivers of active rhizosphere bacterial community dynamics during short-term drought. Nat. Commun. 15, 6347. https://doi.org/10.1038/s41467-024-50463-1.

Byrt, C.S., Millar, A.H., Munns, R., 2023. Staple crops equipped for alkaline soils. Nat. Biotechnol. 41, 911–912. https://doi.org/10.1038/s41587-023-01832-6.

Cha, S., Kim, Y.S., Lee, A.L., et al., 2021. Liming alters the soil microbial community and extracellular enzymatic activities in temperate coniferous forests. Forests 12, 190. https://doi.org/10.3390/f12020190.

Chen, S., Cade-Menun, B.J., Bainard, L.D., et al., 2021. The influence of long-term n and p fertilization on soil p forms and cycling in a wheat/fallow cropping system. Geoderma 404. https://doi.org/10.1016/j.geoderma.2021.115274.

Chen, X.D., Jiang, N., Condron, L.M., et al., 2019. Impact of long-term phosphorus fertilizer inputs on bacterial *phod* gene community in a maize field, northeast China. Sci. Total Environ. 669, 1011–1018. https://doi.org/10.1016/j.scitotenv.2019.03.172.

Chen, G.L., Xiao, L., Yue, K., et al., 2025. Optimizing phosphate application to improve soil quality and reduce phosphorus loss in rice-wheat rotation. Agric. Ecosyst. Environ. 378, 109310. https://doi.org/10.1016/j.agee.2024.109310.

Deinert, L., Hossen, S., Ikoyi, I., et al., 2024. Poultry litter biochar soil amendment affects microbial community structures, promotes phosphorus cycling and growth of barley (Hordeum vulgare). Eur. J. Soil Biol. 120, 103591. https://doi.org/10.1016/j.ejsobi.2023.103591.

Fang, C., Du, H.P., Wang, L.S., et al., 2024. Mechanisms underlying key agronomic traits and implications for molecular breeding in soybean. J. Genet. Genom. 51, 379–393. https://doi.org/10.1016/j.jgg.2023.09.004.

Feng, Y., He, J., Zhang, H.C., et al., 2024. Phosphate solubilizing microorganisms: a sustainability strategy to improve urban ecosystems. Front. Microbiol. 14, 1320853. https://doi.org/10.3389/fmicb.2023.1320853.

Fink, J., Borga, G., Frosi, G., et al., 2020. Enhancing wheat and soybean yields in a subtropical oxisol through effective p fertilization strategies. J. Soil Sci. Plant Nutr. 20, 1–9. https://doi.org/10.1007/s42729-020-00232-y.

Fu, S.F., Balasubramanian, V.K., Chen, C.L., et al., 2024. The phosphate-solubilising fungi in sustainable agriculture: unleashing the potential of fungal biofertilisers for plant growth. Folia Microbiol. 69, 697–712. https://doi.org/10.1007/s12223-024-01181-0.

Gao, Y., Shao, G.C., Yang, Z., et al., 2021. Influences of soil and biochar properties and amount of biochar and fertilizer on the performance of biochar in improving plant photosynthetic rate: a meta-analysis. Eur. J. Agron. 130, 126345. https://doi.org/10.1016/j.eja.2021.126345.

Gong, H.Q., Meng, F.L., Wang, G.H., et al., 2022. Toward the sustainable use of mineral phosphorus fertilizers for crop production in China: from primary resource demand to final agricultural use. Sci. Total Environ. 804, 150183. https://doi.org/10.1016/j.scitotenv.2021.150183.

Guo, S.B., Zhang, Z.T., Guo, E., et al., 2022. Historical and projected impacts of climate change and technology on soybean yield in China. Agric. Sys. 203, 103522. https://doi.org/10.1016/j.agsy.2022.103522.

Harter, J., Krause, H.-M., Schuettler, S., et al., 2013. Linking N_2O emissions from biochar-amended soil to the structure and function of the N-cycling microbial community. ISME J. 8, 660–674. https://doi.org/10.1038/ismej.2013.160.

Hong, C., Lu, S.G., 2018. Does biochar affect the availability and chemical fractionation of phosphate in soils? Environ. Sci. Pollut. Res. Int. 25, 8725–8734. https://doi.org/10.1007/s11356-018-1219-8.

Hossain, M.Z., Bahar, M.M., Sarkar, B., et al., 2020. Biochar and its importance on nutrient dynamics in soil and plant. Biochar 2, 379–420. https://doi.org/10.1007/s42773-020-00065-z.

Huang, Y.L., Dai, Z.M., Lin, J.H., et al., 2021. Contrasting effects of carbon source recalcitrance on soil phosphorus availability and communities of phosphorus solubilizing microorganisms. J. Environ. Manag. 298, 113426. https://doi.org/10.1016/j.jenvman.2021.113426.

Ji, G.Y., Xing, Y.C., You, T.Y., 2024. Biochar as adsorbents for environmental microplastics and nanoplastics removal. J. Environ. Chem. Eng. 12, 113377. https://doi.org/10.1016/j.jece.2024.113377.

Li, B.T., Huang, S., Wang, H.M., et al., 2021. Effects of plastic particles on germination and growth of soybean (Glycine max): a pot experiment under field condition. Environ. Pollut. 272, 116418. https://doi.org/10.1016/j.envpol.2020.116418.

Li, H.Y., Wang, L.H., Zhang, Z.W., et al., 2022. Effect of phosphorus supply levels on nodule nitrogen fixation and nitrogen accumulation in soybean (Glycine max L.). Agronomy 12, 2802. https://doi.org/10.3390/agronomy12112802.

Liao, W.X., Halim, M.A., Kayes, I., et al., 2023. Biochar benefits Green infrastructure: global meta-analysis and synthesis. Environ. Sci. Technol. 57, 15475–15486. https://doi.org/10.1021/acs.est.3c04185.

Liu, C.J., Gong, X.W., Dang, K., et al., 2020. Linkages between nutrient ratio and the microbial community in rhizosphere soil following fertilizer management. Environ. Res. 184, 109261. https://doi.org/10.1016/j.envres.2020.109261.

Liu, Y.F., He, B.P., Xiao, Q.Q., et al., 2023. Earthworms facilitated pepper (Capsicum annuum L.) growth via enhancing the population and function of arbuscular mycorrhizal fungi in a low-density polyethylene-contaminated soil. Chem. Biol. Technol. Agric. 10, 115. https://doi.org/10.1186/s40538-023-00493-6.

Liu, Y.Q., Wen, Y.J., Cai, H.X., et al., 2025. Stress of polyethylene and polylactic acid microplastics on pakchoi (Brassica rapa subsp. chinensis) and soil bacteria: biochar mitigation. J. Hazard. Mater. 487, 137301. https://doi.org/10.1016/j.Jhazmat.2025.137301.

Liu, M.L., Zhao, M.Z., Yang, G., et al., 2024. Root morphology, nitrogen metabolism and amino acid metabolism in soybean under low phosphorus stress. Sci. Rep. 14, 28583. https://doi.org/10.1038/s41598-024-79876-0.

Lu, J.Y., Cai, J.P., Dijkstra, F.A., et al., 2024. Rhizosphere priming and effects on mobilization and immobilization of multiple soil nutrients. Soil Biol. Biochem 199, 109615. https://doi.org/10.1016/j.soilbio.2024.109615.

Ma, X.F., Wei, Z.J., Wang, X.M., et al., 2024. Microplastics from polyvinyl chloride agricultural plastic films do not change nitrogenous gas emission but enhance denitrification potential. J. Hazard. Mater. 479, 135758. https://doi.org/10.1016/j.jhazmat.2024.135758.

Marcos, V., S. E, L.M., Jaime, N., et al., 2023. Nematophagous fungi: a review of their phosphorus solubilization potential. Microorganisms 11, 137. https://doi.org/10.3390/microorganisms11010137.

Mitchell, P.J., Simpson, A.J., Soong, R., et al., 2016. Biochar amendment and phosphorus fertilization altered forest soil microbial community and native soil organic matter molecular composition. Biogeochemistry 130, 227–245. https://doi.org/10.1007/s10533-016-0254-0.

Mo, X.H., Liu, G.X., Zhang, Z.Y., et al., 2022. Mechanisms underlying soybean response to phosphorus deficiency through integration of omics analysis. Int. J. Mol. Sci. 23, 4592. https://doi.org/10.3390/ijms23094592.

Ning, Q., Chen, L., Zhang, C.Z., et al., 2021. Saprotrophic fungal communities in arable soils are strongly associated with soil fertility and stoichiometry. Appl. Soil Ecol. 159, 103843. https://doi.org/10.1016/j.apsoil.2020.103843.

Niroshika, P.K., Kyung, S.M., Deshani, I.A., et al., 2022. Biochar alters chemical and microbial properties of microplastic-contaminated soil. Environ. Res. 209, 112807. https://doi.org/10.1016/j.envres.2022.112807.

Palansooriya, K.N., Sang, M.K., El-Naggar, A., et al., 2023. Low-density polyethylene microplastics alter chemical properties and microbial communities in agricultural soil. Sci. Rep. 13, 16276. https://doi.org/10.1038/s41598-023-42285-w.

Prabhu, N., Borkar, S., Garg, S., 2018. Phosphate solubilization mechanisms in alkaliphilic bacterium *bacillus marisflavi* FA7. Curr. Sci. 845–853. https://doi.org/10.18520/cs/v114/i04/845-853.

Shi, Y.X.X., Yu, Y.C., Chang, E., et al., 2023. Effect of biochar incorporation on phosphorus supplementation and availability in soil: a review. J. Soils Sediment. 23, 672–686. https://doi.org/10.1007/s11368-022-03359-w.

Spina, F., Tummino, M.L., Poli, A., et al., 2021. Low density polyethylene degradation by filamentous fungi. Environ. Pollut. 274, 116548. https://doi.org/10.1016/j.envpol.2021.116548.

Tesfaye, F., Liu, X.Y., Zheng, J.F., et al., 2021. Could biochar amendment be a tool to improve soil availability and plant uptake of phosphorus? A meta-analysis of published experiments. Environ. Sci. Pollut. Res. Int. 28, 34108–34120. https://doi.org/10.1007/s11356-021-14119-7.

Thompson, R.C., Olsen, Y., Mitchell, R.P., et al., 2004. Lost at sea: where is all the plastic? Science 304, 838. https://doi.org/10.1126/science.1094559.

Tian, J.H., Kuang, X.Z., Tang, M.T., et al., 2021. Biochar application under low phosphorus input promotes soil organic phosphorus mineralization by shifting bacterial *phod* gene community composition. Sci. Total Environ. 779, 146556. https://doi.org/10.1016/j.scitotenv.2021.146556.

Tian, J.H., Lu, X., Chen, Q.Q., et al., 2022. Phosphorus fertilization affects soybean rhizosphere phosphorus dynamics and the bacterial community in karst soils. Plant Soil 475, 137–152. https://doi.org/10.1007/s11104-020-04662-6.

Wang, R., Lin, F.Q., Feng, K., 2024. Soybean overweight shock (SOS): the impact of trade liberalization in China on overweight prevalence. China Econ. Rev. 87, 102224. https://doi.org/10.1016/j.chieco.2024.102224.

Wang, R.T., Tu, Z., Qi, C.H., et al., 2024. Copyrolysis of biomass with $Ca_3(PO_4)_2$ and MgO for loading enterobacter hormaechei Wu15 to promote pea growth in saline–alkali soil. ACS Sustain. Chem. Eng. 12, 5010–5022. https://doi.org/10.1021/acssuschemeng.4c00135.

Wang, J.C., Zhu, Y.G., Ge, Y., 2024. Global distribution pattern of soil phosphorus-cycling microbes under the influence of human activities. Glob. Change Biol. 30, e17477. https://doi.org/10.1111/gcb.17477.

Wu, L.K., Wang, J.Y., Huang, W.M., et al., 2015. Plant-microbe rhizosphere interactions mediated by rehmannia glutinosa root exudates under consecutive monoculture. Sci. Rep. 5, 15871. https://doi.org/10.1038/srep15871.

Wu, D., Zhang, W.M., Xiu, L.Q., et al., 2022. Soybean yield response of biochar-regulated soil properties and root growth strategy. Agronomy 12, 1412. https://doi.org/10.3390/agronomy12061412.

Xu, Z.M., Fosu, K.A., Wang, H.L., et al., 2024. Interactive effects of biochar and phosphorus fertilizer on *phod*-harboring bacteria and phosphorus dynamics in moso bamboo forest soil. J. Soil Sci. Plant Nutr. 24, 1–14. https://doi.org/10.1007/s42729-024-02020-4.

Xu, H.R., Liu, W.D., He, Y.H., et al., 2025. Plant-root microbiota interactions in nutrient utilization. Front. Agric. Sci. Eng. 12, 16–26. https://doi.org/10.15302/J-FASE-2024595.

Xu, J., Liu, S.J., Song, S.R., et al., 2018. Arbuscular mycorrhizal fungi influence decomposition and the associated soil microbial community under different soil phosphorus availability. Soil Biol. Biochem 120, 181–190. https://doi.org/10.1016/j.soilbio.2018.02.010.

Yan, T.T., Xue, J.H., Zhou, Z.D., et al., 2021. Biochar-based fertilizer amendments improve the soil microbial community structure in a karst mountainous area. Sci. Total Environ. 794, 148757. https://doi.org/10.1016/j.scitotenv.2021.148757.

Ye, L., Camps-Arbestain, M., Shen, Q., et al., 2020. Biochar effects on crop yields with and without fertilizer: a meta-analysis of field studies using separate controls. Soil Use Manag. 36, 2–18. https://doi.org/10.1111/sum.12546.

Zhang, L.X., Chang, L., Liu, H.J., et al., 2025. Biochar application to soils can regulate soil phosphorus availability: a review. Biochar 7, 13. https://doi.org/10.1007/s42773-024-00415-1.

Zhang, Z., Fan, X.X., Zhang, R.M., et al., 2025. Biodegradation characterization and mechanism of low-density polyethylene by the enriched mixed-culture from plastic-contaminated soil. J. Hazard. Mater. 494, 138530. https://doi.org/10.1016/j.jhazmat.2025.138530.

Zhang, L., Guo, K., Wang, L., et al., 2022. Effect of sludge retention time on microbial succession and assembly in thermal hydrolysis pretreated sludge digesters: deterministic versus stochastic processes. Water Res. 209, 117900. https://doi.org/10.1016/j.watres.2021.117900.

Zhang, Z.K., Zhao, L., Jin, Q.W., et al., 2024. Combined contamination of microplastic and antibiotic alters the composition of microbial community and metabolism in wheat and maize rhizosphere soil. J. Hazard. Mater. 473, 134618. https://doi.org/10.1016/j.jhazmat.2024.134618.

Zhang, K., Zheng, D.F., Gu, Y., et al., 2023. Utilizing soil organic phosphorus for sustainable crop production: insights into the rhizosphere. Plant Soil 498, 57–75. https://doi.org/10.1007/s11104-023-06136-x.

Zhao, S.W., Zhang, Q.R., Chen, X.M., et al., 2025. Biochar counteracts the negative effects of microplastics on physiological and biochemical characteristics and leaf metabolism in zea mays l. J. Hazard. Mater. 496, 139355. https://doi.org/10.1016/j.jhazmat.2025.139355.

Zhu, F., Zhang, X.C., Guo, X.Y., et al., 2023. Root architectures differentiate the composition of organic carbon in bauxite residue during natural vegetation. Sci. Total Environ. 883, 163588. https://doi.org/10.1016/j.scitotenv.2023.163588.

Zwetsloot, M.J., Lehmann, J., Bauerle, T., et al., 2016. Phosphorus availability from bone char in a P-fixing soil influenced by root-mycorrhizae-biochar interactions. Plant Soil 408, 95–105. https://doi.org/10.1007/s11104-016-2905-2.